

The preliminary experimental results of high-field-side divertor target biasing system (HDTB) on J-TEXT

Qinghu Yang¹, Zhipeng Chen^{1,*}, Yihan Wang¹, Jinlong Guo¹ and J-TEXT team^{1,†}

¹ *International Joint Research Laboratory of Magnetic Confinement Fusion and Plasma Physics, State Key Laboratory of Advanced Electromagnetic Technology, Huazhong University of Science and Technology, Wuhan, China*

* Corresponding author: zpchen@hust.edu.cn

† See Ding et al 2024 (<https://doi.org/10.1088/1741-4326/ad336e>) for the J-TEXT team.

Abstract

Recently, a toroidally quasi-symmetric distributed high-field-side divertor target biasing (HDTB) system has been newly installed on the J-TEXT tokamak. Experiments on HDTB were conducted under the high-field-side mid-single null (HFS-MSN) divertor configuration in J-TEXT. In the unique floating hybrid biasing mode (FHB), both $\mathbf{E}_r \times \mathbf{B}$ poloidal flow and $\mathbf{E}_\theta \times \mathbf{B}$ radial flow were simultaneously driven, modulating the up-down asymmetry distribution of strike point parameters and effectively broadening the particle flow distribution in the scrape-off layer (SOL) region. Additionally, target biasing also influenced impurity distribution in the SOL region, showing potential for achieving detachment by active modulation of impurity radiation.

1. The HDTB system

The $\mathbf{E} \times \mathbf{B}$ drift is considered a key factor affecting the distribution of particles and heat flux in the divertor boundary^[2]. Therefore, by actively altering the potential distribution using external bias voltage, the $\mathbf{E} \times \mathbf{B}$ flow at the boundary can be controlled. This idea has been implemented in many devices such as TdeV^[3], DIII-D^[4], etc., where divertor target biasing significantly modified particle and heat flux distributions, impurity screening, and other parameters. The J-TEXT tokamak features a unique high-field-side mid-single null (HFS-MSN) configuration^[1], as shown in Figure 1(a). This eliminates the influence of geometric factors on strike point parameters, making it an ideal platform for conducting divertor target biasing experiments.

The high-field-side divertor target biasing (HDTB) system of the J-TEXT is updated from the divertor target, as shown in Figure 1(b). The biased target plates nearly cover a full toroidal loop to achieve a larger biasing area. The system consists of upper and down

target plate arrays. The upper biased target (UBT) array is entirely located in the SOL region, while the down biased target (DBT) covers the down strike point and extends into the private flux region (PFR). The two arrays are asymmetrically distributed along the midplane, meaning the magnetic flux tubes connecting them are misaligned in the magnetic surface coordinate system, as illustrated in Figure 1(c). Previous electromagnetic simulation results^[5] indicate that under reversed toroidal field conditions ($\mathbf{B} \times \nabla \mathbf{B}$ upward), applying a positive bias voltage between the UBT and DBT can drive an $\mathbf{E}_r \times \mathbf{B}$ poloidal flow toward the upper divertor, mitigating the asymmetric distribution of strike point parameters, while also driving an outward $\mathbf{E}_\theta \times \mathbf{B}$ radial flow to broaden the SOL region. Since UBT and DBT are connected to the power supply's two poles without grounding, this biasing mode is referred to as the floating hybrid biasing mode (FHB). Preliminary experimental results based on this FHB mode will be presented below.

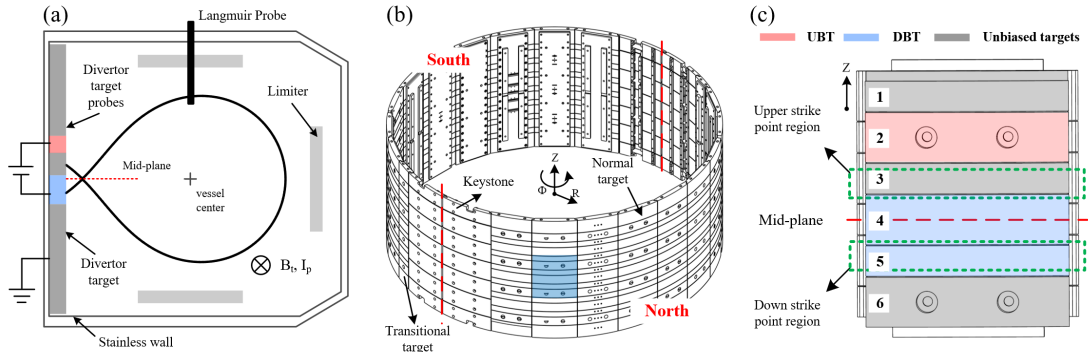


Figure 1. (a) Poloidal cross-section of the J-TEXT tokamak, the black curve represents the separatrix of the mid-single null divertor configuration; (b) distribution map of the HFS divertor targets. (c) Partial detail of the J-TEXT HFS divertor target, the green dashed box indicates the divertor strike point region.

2. Preliminary experimental results of FHB mode

The experiment was conducted in the HFS-MSN divertor configuration. The power supply's two poles were connected to the UBT and DBT, respectively, with $\pm 100V$ bias voltages applied. The upstream and downstream plasma parameter profiles were measured by the reciprocating combined Langmuir-magnetic probe (CLMP) and the HFS divertor target probe array, respectively. During biasing, the plasma potentials V_p at the upstream and downstream were significantly modulated, as shown in Figures 2(a) and 2(b). Under positive bias, the radial electric field E_r in the SOL region ($r - r_{sep} = 0 \sim 0.02m$) was significantly reduced or even reversed, while negative bias enhanced the outward \mathbf{E}_r in the SOL, as illustrated in Figure 2(c). Unfortunately, the poloidal electric field \mathbf{E}_θ distribution was not directly measured. The \mathbf{E}_r and \mathbf{E}_θ driven by the +100V FHB, along with the corresponding $\mathbf{E}_r \times \mathbf{B}$ and $\mathbf{E}_\theta \times \mathbf{B}$ drift direction, are depicted in Figure 2(d).

Positive bias effectively broadens the distribution of ion saturation current J_s and parallel heat flux Q_{\parallel} in the upstream SOL region, while negative bias makes the distribution more peaked, as shown in Figure 3(a) and (c). The bias also alters the asymmetry of J_s and Q_{\parallel} near the upper and down strike points. Positive bias increases particle and heat fluxes at the down divertor, whereas negative bias has the opposite effect, as illustrated in Figure (b) and (d). The changes in upstream and downstream parameter profiles are consistent with the direction of the $\mathbf{E}_r \times \mathbf{B}$ and $\mathbf{E}_\theta \times \mathbf{B}$ flows driven by the HDTB.

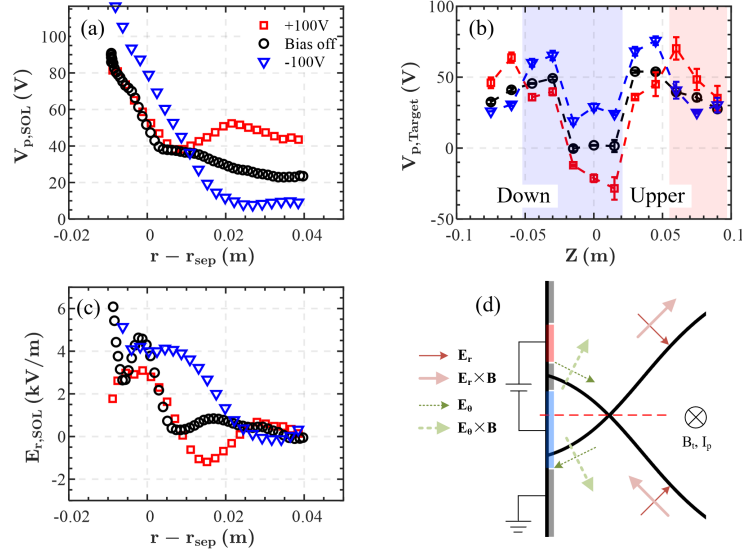


Figure 2. Upstream and downstream plasma potential V_p profiles (a-b); upstream radial electric field E_r profiles (c); the directions of the \mathbf{E}_r and \mathbf{E}_θ , along with the corresponding $\mathbf{E}_r \times \mathbf{B}$ poloidal and $\mathbf{E}_\theta \times \mathbf{B}$ radial flow in SOL under positive FHB mode (d).

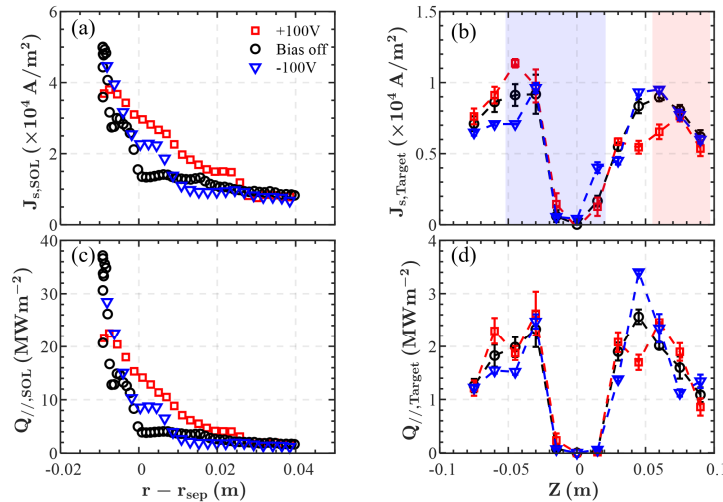


Figure 3. Upstream and downstream ion saturation current density J_s (a-b); parallel heat flux Q_{\parallel} (c-d) profiles.

Additionally, the HDTB also affects the distribution of impurity radiation, as shown in Figure 4(a-c). Without biasing, the CIII radiation observed by the CCD (equipped with a CIII filter) is stronger in the down divertor. Positive bias further increases this asymmetry,

while negative bias enhances the overall impurity radiation, with a more significant increase in the upper divertor region. A reasonable target plate bias setting is conducive to achieving detachment. The CIII array measurements from the PDA are consistent with the CCD measurements, as shown in Figure 4(e). The H_α array of the PDA covers the upper divertor region, observing a significant enhancement in H_α radiation under negative bias, as shown in figure 4(d), which aligns with probe measurements.

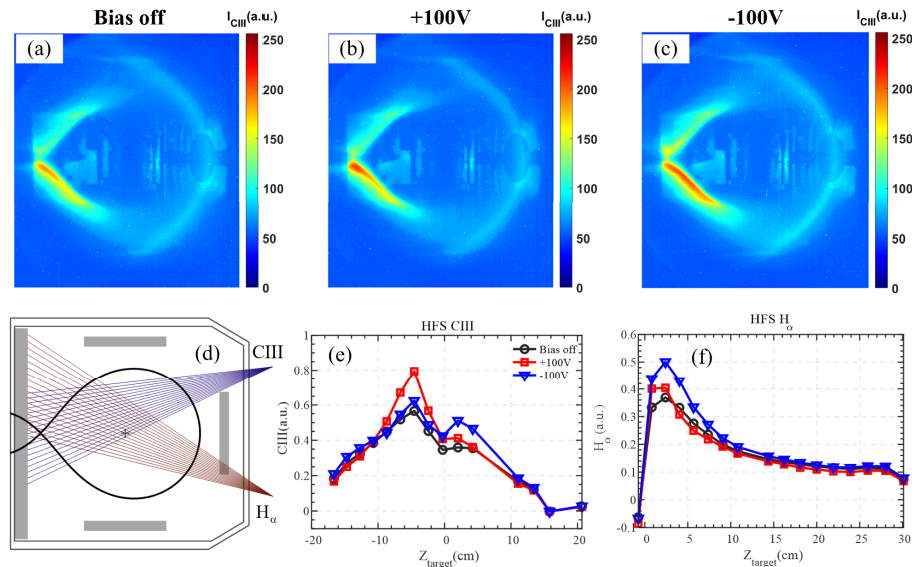


Figure 4. The distribution of CIII impurity radiation observed by CCD (a-c); schematic diagram of PDA array (d), and the distribution of CIII and H_α radiation measured by PDA array.

3. Summary and Acknowledge

The high-field-side divertor target biasing (HDTB) system has been successfully implemented in the J-TEXT tokamak. Preliminary experimental results indicate that the unique floating hybrid biasing (FHB) mode can effectively modulate the asymmetry of particle flux, heat flux, and impurity radiation distribution near the strike points, while simultaneously broadening the SOL region, achieving the intended experimental objectives.

This work was supported by Natural Science Foundation of China (NSFC) under Project Numbers Grant (Nos. 12275098), and Hubei International Science and Technology Cooperation Projects (No. 2022EHB003).

References

- [1] Z. Chen, *et al.*, *Plasma Sci. Technol.* **24**, 124008 (2022).
- [2] A. V. Chankin. *Journal of Nuclear Materials* **241–243**, 199–213 (1997).
- [3] A. Boileau. *Nucl. Fusion* **33**, 1627–1633 (1993).
- [4] M. J. Schaffer, *Nucl. Fusion* **36**, 495 (1996).
- [5] J. Guo, *2024 IEEE China International Youth Conference on Electrical Engineering*, pp. 1–6.